Paleobiology

cambridge.org/pab

Functional morphology of the Ediacaran organism *Tribrachidium heraldicum*

A. Olaru[1], S. Gutarra-Diaz[2], R. A. Racicot[1,3], F. S. Dunn[4], I. A. Rahman[2,4], Z. Wang[2], S. A. F. Darroch[1,3] and B. M. Gibson[1]

[1]Vanderbilt University, Earth and Environmental Sciences, Nashville, Tennessee, U.S.A.
[2]Natural History Museum, London, U.K.
[3]Senckenberg Gesellschaft für Naturforschung, Frankfurt am Main, Hessen Germany
[4]Oxford University Museum of Natural History, Oxford, Oxfordshire, U.K.

Article

Cite this article: Olaru A, Gutarra-Diaz S, Racicot RA, Dunn FS, Rahman IA, Wang Z, Darroch SAF, Gibson BM (2024). Functional morphology of the Ediacaran organism *Tribrachidium heraldicum*. *Paleobiology* 1–15. https://doi.org/10.1017/pab.2024.24

Received: 26 July 2023
Revised: 24 July 2024
Accepted: 6 August 2024

Corresponding author:
B. M. Gibson;
Email: brandt.m.gibson@vanderbilt.edu

Non-technical Summary

Tribrachidium heraldicum is among the first large and structurally complex animals, appearing in the fossil record 550 million years ago. By using engineering software to simulate fluid flow around digital models of this organism, we recreate details of how it lived, including how it fed and the likely functions of its bizarre anatomy.

Abstract

Tribrachidium heraldicum is an Ediacaran body fossil characterized by triradial symmetry. Previous work has suggested that the anatomy of *Tribrachidium* was conducive to passive suspension feeding; however, these analyses used an inaccurate model and a relatively simple set of simulations. Using computational fluid dynamics, we explore the functional morphology of *Tribrachidium* in unprecedented detail by gauging how the presence or absence of distinctive anatomical features (e.g., apical pits and arms) affects flow patterns. Additionally, we map particle pathways, quantify deposition rates at proposed feeding sites, and assess gregarious feeding habits to more fully reconstruct the lifestyle of this enigmatic taxon. Our results provide strong support for interpreting *Tribrachidium* as a macroscopic suspension feeder, with the apical pits representing loci of particle collection (and possibly ingestion) and the triradial arms representing morphological adaptations for interrupting flow and inducing settling. More speculatively, we suggest that the radial grooves may represent ciliated pathways through which food particles accumulating in the wake of the organism were transported toward the apical pits. Finally, our results allow us to generate new functional hypotheses for other Ediacaran taxa with a triradial body plan. This work refines our understanding of the appearance of suspension feeding in shallow-water paleoenvironments, with implications for the radiation of Metazoa across the Ediacaran/Cambrian boundary.

Introduction

Suspension feeding is a crucial process in modern oceans, decreasing the concentration of organic particles and phytoplankton in the water column and allowing for more efficient transport and burial of organic carbon in shallow-marine environments (Gili and Coma 1998). In turn, this helps to form energetic links between the benthic and pelagic realms while also reducing primary productivity (Gili and Coma 1998; Wood and Curtis 2014). The appearance of the first macroscopic suspension feeders in the late Ediacaran (Wood and Curtis 2014; Rahman et al. 2015; Darroch et al. 2018) is therefore expected to have had profound effects on ecosystem structure and biodiversity during the emergence of animals, potentially helping "fuel" the radiation of more energetically intensive metazoan behaviors over the Ediacaran/Cambrian transition (Rahman et al. 2015; Lerosey-Aubril and Pates 2018; Cracknell et al. 2021; Darroch et al. 2022). In this context, the Ediacaran-aged organism *Tribrachidium heraldicum* is crucial, as it has been suggested that it represents one of the earliest macroscopic suspension feeders in shallow-marine environments (Rahman et al. 2015; Hall et al. 2020; though see Butterfield 2022). Moreover, it is part of a larger group of organisms with radial symmetry that are thought to have fed in a similar fashion, indicating that benthic suspension feeding may have been widespread by the late Ediacaran (Cracknell et al. 2021). In this paper, we analyze the functional morphology of *Tribrachidium* using computational fluid dynamics (CFD) with the goal of testing to what extent specific anatomical features may represent adaptations for suspension feeding. This provides a character-based framework with which to infer the feeding mode of other Ediacaran-aged radial taxa that underwent rapid diversification as part of the "second wave" of Ediacaran evolution (Droser and Gehling 2015; Hall et al. 2015) and may thus have had a profound influence on patterns of energy flow through benthic communities (Rahman et al. 2015).

PALEOBIOLOGY A PUBLICATION OF THE Paleontological SOCIETY

CAMBRIDGE UNIVERSITY PRESS

Tribrachidium heraldicum is restricted to the "White Sea" interval of the late Ediacaran (~558–550 Ma) (Waggoner 2003; Boag et al. 2016), which is best known from fossil assemblages in South Australia and Russia. It is characterized by an unusual triradial body architecture that differs from that of any extant animal phyla (Hall et al. 2015, 2020; Rahman et al. 2015; Ivantsov and Zakrevskaya 2021). *Tribrachidium* is a broadly hemispherical or "dome-shaped" organism, ~2–4 cm in diameter, with three curved "arms" that meet at the apex, spiral clockwise down the sides of the body, and become parallel to the organism's perimeter at its margin (e.g., Hall et al. 2015; Fig. 1). In between the arms are three evenly distributed pit-like depressions, termed "apical pits" by Rahman et al. (2015). Near the midpoint of each curving arm are bulbous structures termed "bullae." Well-preserved specimens also exhibit a "tentacular fringe" that has been interpreted as a secondary branching structure (Hall et al. 2015).

Tribrachidium belongs to the Triradialomorpha (Hall et al. 2015), an informal grouping of Ediacaran-aged taxa characterized by triradial symmetry (Hall et al. 2020; see also Fedonkin [1985] for a similar proposed grouping). However, it is unique among triradialomorphs in possessing curved (rather than straight or branching) surface features, and it is notable for its abundance in White Sea fossil deposits recording a variety of shallow-marine depositional environments within or just below storm wave base (Fedonkin 1985; Gehling and Droser 2013; Grazhdankin 2014; Hall et al. 2020). In Nilpena (South Australia) alone, *Tribrachidium* is found in four of the five facies present in the exposed sections—shoreface sands, wave-base sands, delta-front sands, and sheet-flow sands (Gehling and Droser 2013)—representing a variety of water depths and hydrodynamic regimes. *Tribrachidium* can also be locally abundant, sometimes representing upward of 60% of individuals on fossil slabs (Hall et al. 2020; Boan et al. 2023), and is thus one of several Ediacaran-aged sessile taxa that may have gained ecological benefits from living in aggregated populations on the seafloor (see e.g., Gibson et al. 2019, 2021a; Darroch et al. 2022), although this has yet to be explicitly tested.

CFD Modeling of Tribrachidium

Rahman et al. (2015) previously reconstructed *Tribrachidium* as a passive suspension feeder on the basis of CFD simulations. Their study used a digital model of *Tribrachidium* obtained via micro-computed tomography scanning and found evidence for redirection of flow by the three spiral arms toward the apical pits. Slow recirculation of fluid within these apical pits was inferred to have allowed particles to fall out of suspension under the influence of gravity, onto a hypothesized collection or filtering apparatus. This mode of passive suspension feeding is termed "gravitational deposition" (LaBarbera 1984), and it is thought to be an important method of nutrient acquisition among several groups of extant marine invertebrates (e.g., Koehl 1977; LaBarbera 1984).

Although the CFD simulations performed by Rahman et al. (2015) represented a significant breakthrough in understanding the functional morphology of *Tribrachidium*, their study had several limitations. First, these authors used a relatively inaccurate model of *Tribrachidium* that was significantly taphonomically deformed. Second, they assumed the path of food particles suspended in water followed streamlines, which does not account for the influence of particle size, mass density, and concentration. Third, they performed analyses using only the complete model and a smooth dome as a null model, and hence could not test the role of specific anatomical features purported to aid in suspension feeding. Finally, their previous model possessed arms that erroneously spiraled counterclockwise rather than clockwise. In this study, we address these limitations and build on the previous work by constructing new, more anatomically accurate digital models of *Tribrachidium* along with a series of hypothetical models with different combinations of key anatomical features. These models are designed to also incorporate the range of preserved anatomies (and thus various reconstructions) observed between Russia and South Australia (Ivantsov and Zakrevskaya 2021), principally in experimenting with both hemispherical and more elongate apical pits (Fig. 1G,H). We use CFD to reconstruct fluid flow around these models, with flow properties informed by sedimentological evidence from Ediacaran-aged fossil localities and hydrological data from equivalent modern environments. We also carry out preliminary semi-resolved computational fluid dynamics–discrete element method (CFD-DEM) simulations (Wang et al. 2019) to reproduce the interactions between fluid flow, solid surfaces (i.e., the organism and the seafloor), and particles with the physical properties of plankton. The results allow us to systematically test how the morphology of *Tribrachidium* controlled patterns of fluid flow and, ultimately, reassess the paleoecological interpretations previously assigned to these flow features. This allows us to better resolve the feeding mode of *Tribrachidium*, with implications for constraining the emergence of suspension feeding and associated Earth systems impacts ~558–550 Ma.

Materials and Methods

Three-Dimensional Model Construction

Three-dimensional digital models of *Tribrachidium* were created as non-uniform rational basis spline geometries using Rhinoceros 3D v. 7. The distance between the apical pits and the center of the body, as well as the manner in which the arms taper to the margin, were recreated from photographs of well-preserved fossil specimens from South Australia (taken from, e.g., Hall et al. [2015]). The result is a "complete" model of *Tribrachidium* that excludes only the tentacular fringe, which was omitted due to computational and modeling constraints. A stepped series of hypothetical models were then constructed by removing specific anatomical features (apical pits, triradial arms, and bullae) from the complete *Tribrachidium* model (Fig. 2). In addition to the South Australian material, we developed a series of models with elongate pits, wider arms, and a less pronounced apical protrusion where the arms converge. This additional set of models more closely matches a small number of fossil specimens recently described from the southeastern White Sea region (Ivantsov and Zakrevskaya 2021). Given the different taphonomic and burial histories present in South Australia and Russian, these two end-member models thus serve as a useful sensitivity test, allowing us to understand the extent to which interpreted flow patterns may be biased by deformation.

All models were scaled to match previously reported sizes (Hall et al. 2015, 2020), with the typical specimen diameter of 2–4 cm averaged to 3 cm. The original height of *Tribrachidium* above the sediment–water interface is poorly constrained, with fossils presumably affected by taphonomic compaction (Rahman et al. 2015; Hall et al. 2020). However, the measured heights of specimens from South Australia show only ~2 mm

https://doi.org/10.1017/pab.2024.24 Published online by Cambridge University Press

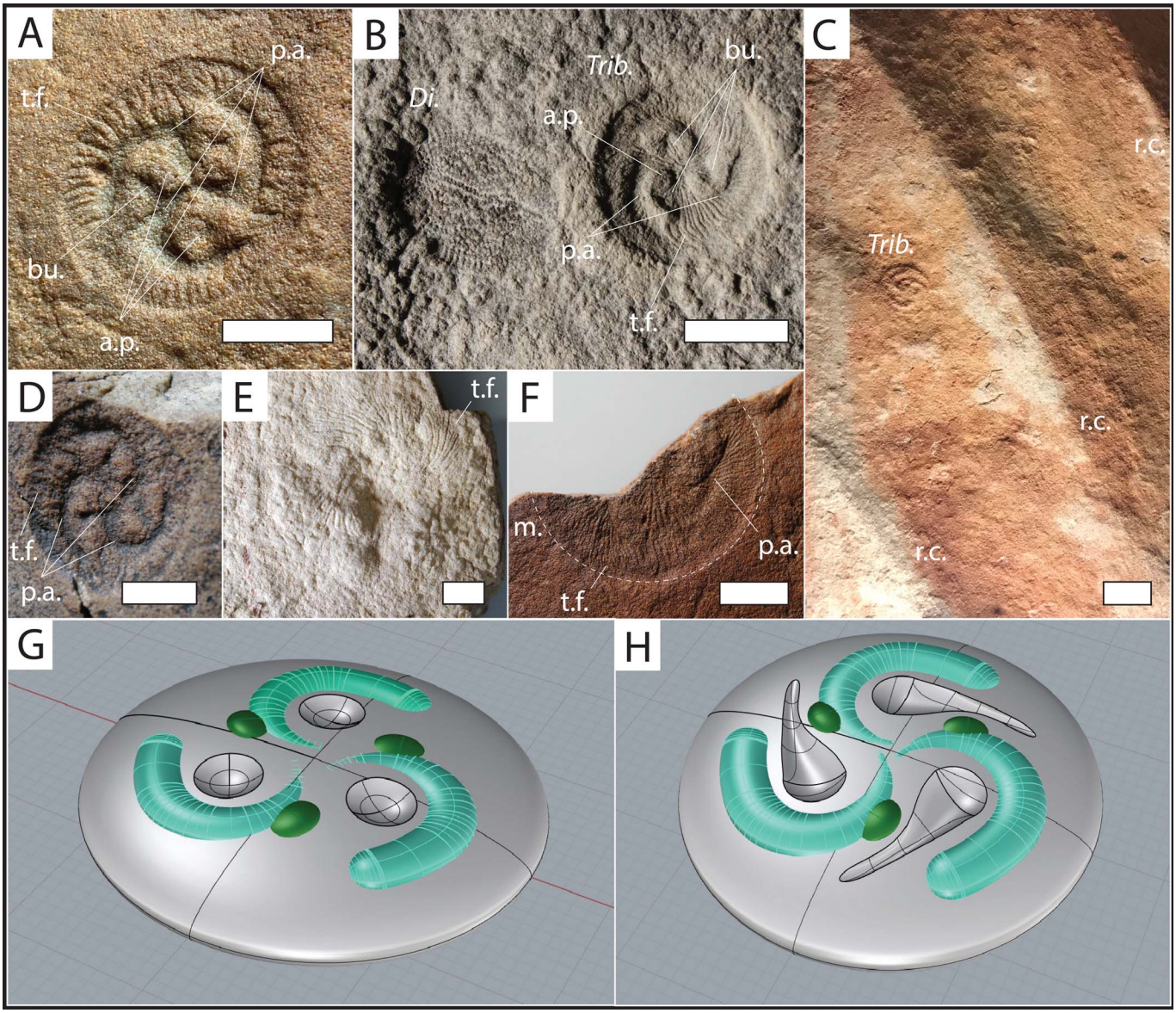

Figure 1. Multi-panel figure illustrating fossil *Tribrachidium* (*Trib.*) from South Australia and Russia, preserved in a range of different styles, and highlighting key anatomical features including the outer margin of the organism (m.), primary arms (p.a.), bullae (bu.), apical pits (a.p.), and tentacular fringe (t.f.). **A,** Holotype specimen SAM P12898 (South Australia Museum). **B,** Specimen N3993/5056 (Palaeontological Institute, Moscow, Russia), preserved next to a small *Dickinsonia* (*Di.*). **C,** Specimen SAM P48718a (South Australia Museum), preserved in the trough between parallel ripple crests (r.c.). **D,** Paratype specimen SAM P12889 (South Australia Museum). **E,** SAM P40876 (South Australia Museum). **F,** Specimen SAM P1020514 (South Australia Museum). **G and H,** Our two "complete" models (primary arms and bullae highlighted in light and dark green, respectively), which contrast hemispherical vs. elongate apical pits, reflecting the potential range of morphologies present in the living organisms. Scale bars, 1 cm.

of scatter (Hall et al. 2020), and thus the degree of compaction is likely to be similar across individuals. Moreover, Rahman et al. (2015) experimented with different model heights, finding that the broad patterns of fluid flow did not change substantially. We therefore chose a single height (3.25 mm) for all our models that reflects the height of the specimen originally scanned by Rahman et al. (2015), allowing for easy comparison with this study.

CFD

CFD simulations were performed in COMSOL Multiphysics v. 6.1 following the methods outlined in Gibson et al. (2021b). Reynolds-averaged Navier-Stokes equations were solved for incompressible flow using the shear stress transport turbulence model. Standard material properties for liquid water [$\rho = 1000\ kg/m^3$, $\mu = 0.001\ kg/(s{\cdot}m)$] were assigned to the flow domain. For all simulations, models were fixed to the lower surface of a hexahedral flow domain (measuring $30 \times 20 \times 5$ cm), which was meshed using a combination of tetrahedral elements in the far field and layers of hexahedral boundary elements near the model and domain floor. Slip wall boundary conditions were applied to all walls parallel to flow, with no-slip conditions assigned to the lower surface of the domain (representing the seafloor) and the *Tribrachidium* model. Opposing inlet/outlet conditions were used to drive flow, where water flow was

https://doi.org/10.1017/pab.2024.24 Published online by Cambridge University Press

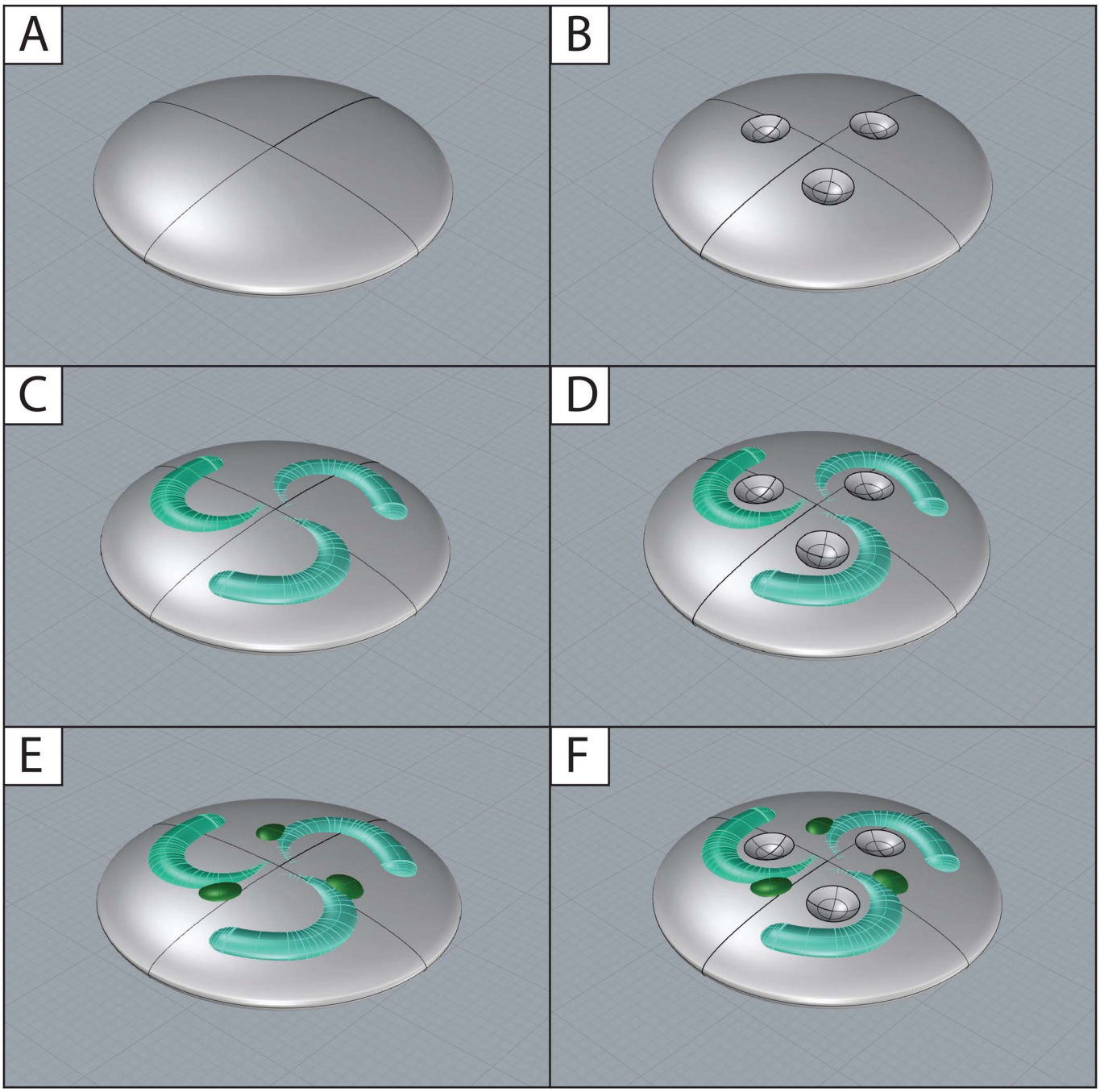

Figure 2. Stepped series of hypothetical digital models of *Tribrachidium* (shown here with hemispherical pits). **A,** Unornamented dome; **B,** dome with apical pits; **C,** dome with triradial arms; **D,** dome with triradial arms and apical pits; **E,** dome with triradial arms and bullae; and, **F,** complete model including triradial arms, apical pits, and bullae.

simulated with a fully developed velocity inlet at the upstream face. Simulations were performed with inlet velocities of 0.05, 0.1, 0.2, and 0.5 m/s, which were chosen to match the typical range of velocities measured in analogous present-day, shoreface environments (Klein and Mittelstaedt 1991; Klein et al. 1999; Darroch et al. 2022). Simulations were conducted with models at three different orientations to flow, 0°, 40°, and 80°. Finally, two mesh refinement sensitivity analyses were undertaken to ensure solutions were independent of mesh element size. As the models based on Russian material from the White Sea area were more geometrically complex, they required finer-resolution meshes.

Group-Level Simulations

To approximate a small population of *Tribrachidium*, we performed CFD simulations with three models in a triangular arrangement (one individual upstream and two individuals downstream). Rahman et al. (2015) previously noted that the radial symmetry of *Tribrachidium* was likely beneficial for

https://doi.org/10.1017/pab.2024.24 Published online by Cambridge University Press

collecting nutrients in all orientations to current; however, their study did not consider the possible influence of wakes produced by upstream individuals, which can have a dramatic impact on benthic communities (see, e.g., Gibson et al. 2019, 2021a). We therefore performed group-level simulations on a triangular arrangement of individuals—where the wake of upstream individuals has an opportunity to disrupt ambient flow around downstream individuals—representing a trade-off between the spectrum of plausible and hydrodynamically "interesting" effects and computational time. For consistency, all models were placed in the 0° orientation. We varied the inter-model distance from almost touching to just less than one model diameter distance between models. Simulations were then performed using the same boundary conditions and meshing parameters as outlined earlier. To quantify results, we integrated drag for individual models in the groups.

CFD-DEM Simulations

We carried out semi-resolved coupled CFD-DEM simulations using CFDEM software (coupled with OpenFOAM and LIGGGHTS). To better capture flow details at the interface between the organism and the fluid, the mesh around the *Tribrachidium* model was refined to be four times smaller than the background mesh in the finite volume method. Due to the limitations of traditional CFD-DEM coupling on the cell/particle size ratio (larger than 3 to accurately reproduce the background flow field), we employed semi-resolved CFD-DEM with kernel approximation (Wang et al. 2019). We also quantified particle–organism interactions, pressure gradient forces, and particle–fluid momentum exchanges such as the drag force, virtual mass force (Zbib et al. 2018), and Magnus force (Mei 1992; Loth and Dorgan 2009).

For CFD-DEM simulations, we used a simulation volume with dimensions of $6 \times 6 \times 3$ cm and a concentration of 13.33 particles/cm^3, where particles had a density of 1080 kg/m^3 and a mean radius of 70 µm (radii [r] ranging from 10 to 250 µm), which is reflective of modern plankton (Dynowski et al. 2016) and on the scale of large-celled phytoplankton present during the latest Neoproterozoic (Brocks et al. 2017; Wang et al. 2018). The turbulence model, boundary conditions, and material properties were otherwise the same as used in the CFD simulations undertaken in COMSOL Multiphysics (see "CFD" section).

A particle outlet was placed at the downstream face of the flow domain, and a particle inlet was placed 3 cm upstream of the *Tribrachidium* model. Particles were instantaneously released spatially at random along a vertical plane (y–z plane) from the left surface of the domain (i.e., the inlet). Particles were released continuously for the duration of the simulation. The initial flow-field conditions were established using a previously solved stationary solution, and the flow field was solved for 20 s leading up to the first release of particles to allow the field to fully develop from the initial conditions.

Results

Although the reconstructed flow patterns varied between different models and orientations to flow, some fundamental aspects of flow were common to all our simulations. Specifically, in parts of the domain far away from the influence of the model, there was a characteristic vertical logarithmic increase in velocity, in agreement with the law of the wall (Schlichting and Gersten 2000). As flow approached the upstream faces of the models, there was a reduction in velocity and a low-velocity wake formed downstream (Figs. 3, 4). In all the simulations, flow around and above the model was slower than the far-field inlet velocity, with the model residing in the laminar to turbulent transitional boundary layer zone. In the following sections, we first describe flow patterns for our stepped series of hypothetical models, reporting how different morphological features impacted small-scale flow patterns. We then describe the effects of changing velocity and orientation on these flow patterns and the results of group-level and CFD-DEM simulations. To illustrate flow patterns at high resolution, we show the results of CFD simulations for our models run at 0.05 and 0.2 m/s in the main text, and 0.1 and 0.5 m/s in the supplementary material.

Hypothetical Models

CFD results for our most basic model—an unornamented dome (Fig. 3A)—showed that flow was evenly distributed over the entire surface of the model, with a low-velocity wake generated downstream. No recirculation was observed in the wake for any of the inlet velocities simulated. With the addition of apical pits, flow patterns were similar, but with a larger wake extending farther downstream for simulations with higher inlet velocities and a greater reduction in velocity downstream of the pits compared with the ambient flow for all simulated inlet velocities. The addition of arms further disrupted flow over and around the model and created a larger, more asymmetrical wake characterized by recirculating flow. This recirculation was redirected by the downstream arm toward the apex of the organism, with patterns strongest at inlet velocities ≥0.1 m/s. When the pits and arms were both included in the model, the arms slowed and redirected flow above the "medial" pit between the upstream and downstream pits, but there was very little reduction in flow velocity or recirculation above the pit that was directly exposed to flow.

Adding the pits and bullae to the arms-only model had little impact on the overall flow patterns, with some small-scale recirculation still evident within the apical pits. However, examining the reconstructed flow patterns at finer scales revealed deviations that were dependent on the presence/absence of particular anatomical features. In the models with arms, the presence of pits noticeably changed the direction and magnitude of flow around the apex of the organism. For example, when comparing the "arms-only" and "arms and pits" models, large-scale flow features like recirculation to the apex were nearly identical, but the arms and pits model exhibited greater velocity magnitudes in small vortices rotating countercurrent to the ambient flow in the inner margins of the arms. This pattern was observed for both the farthest upstream and downstream apical pits that were buffered from flow by the arms. Similar results could be seen when comparing the complete model (which has pits) and the "arms and bullae" model (which lacks pits) (Fig. 5). Comparisons between the simulations with models that included or lacked bullae showed very similar flow patterns, with only slightly different flow directionality around the apex, suggesting that the bullae exerted less control on flow patterns compared with other anatomical features. Furthermore, when the pits were present, flow within them moved countercurrent to the ambient flow direction (Fig. 5). For the models lacking pits, flow in this region still moved in a different direction relative to ambient flow, but the strength of this recirculated current was weaker.

https://doi.org/10.1017/pab.2024.24 Published online by Cambridge University Press

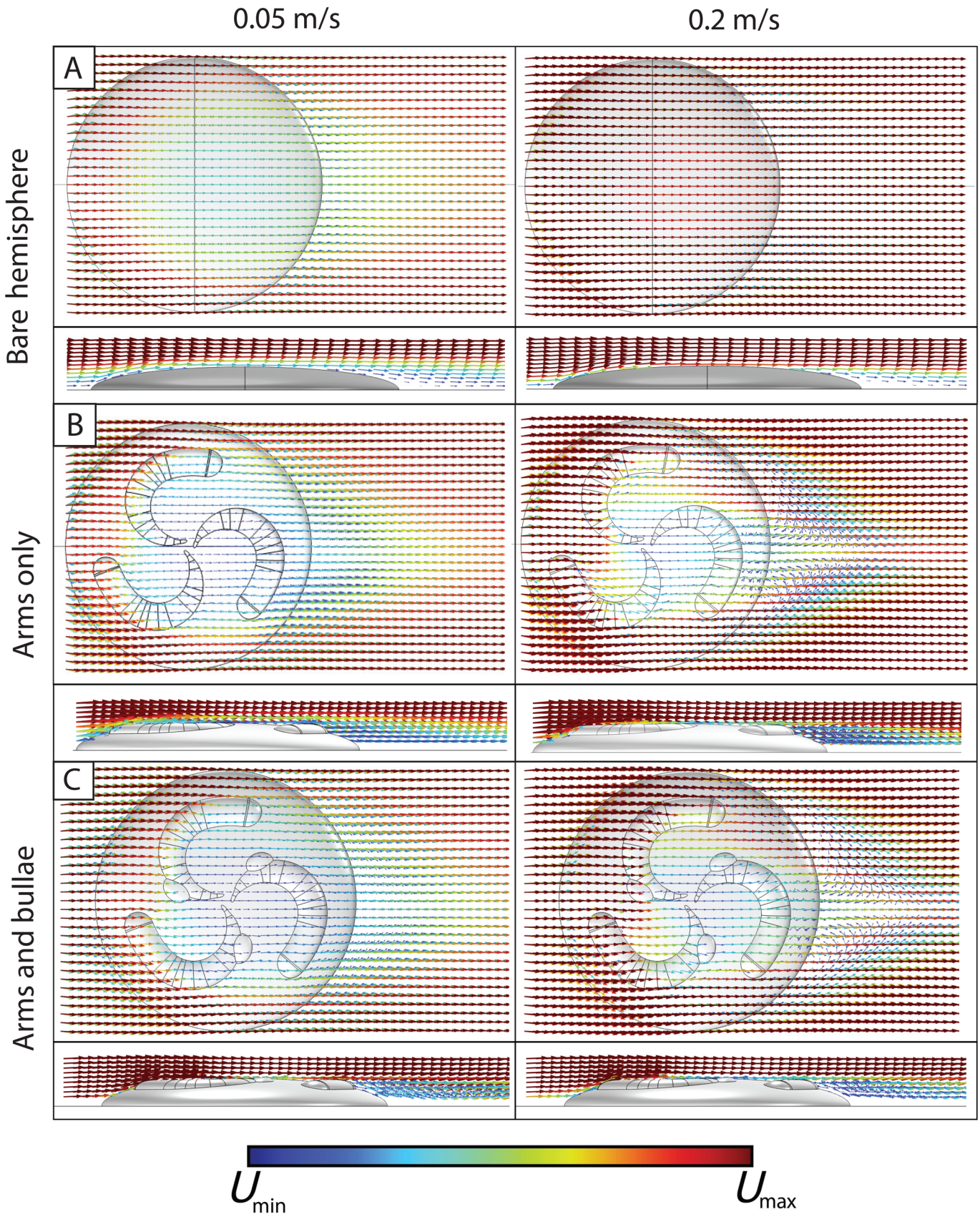

Figure 3. Multi-panel figure illustrating patterns of fluid flow around our hypothetical models of *Tribrachidium* without apical pits: **A,** simple dome; **B,** arms only; and **C,** arms and bullae. Panels show simulations run at 0.05 m/s (left column), and 0.2 m/s (right column); results for simulations run at 0.1 and 0.5 m/s given in the supplementary material. Results visualized as two-dimensional plots of flow-velocity magnitude with flow vectors (rainbow arrows; length of arrows scaled to 8× and 1.5× the flow-velocity magnitude for 0.05 and 0.2 m/s, respectively), in plan (upper panels) and lateral (lower panels) views. The ambient flow is from left to right.

https://doi.org/10.1017/pab.2024.24 Published online by Cambridge University Press

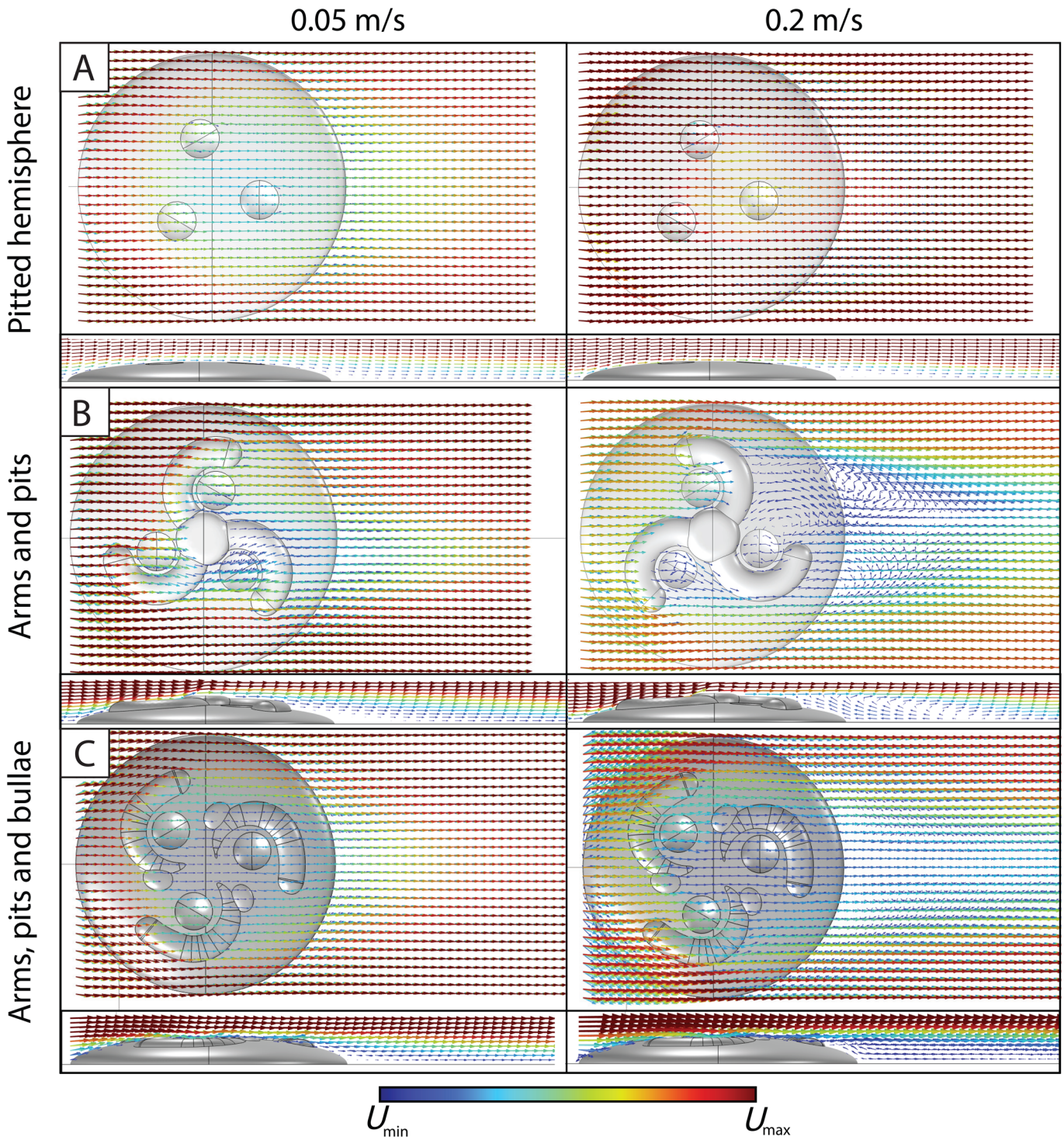

Figure 4. Multi-panel figure illustrating patterns of fluid flow around our hypothetical models of *Tribrachidium* with apical pits: **A,** pitted dome; **B,** arms and pits; and **C,** arms, pits, and bullae. Panels show simulations run at 0.05 m/s (left column) and 0.2 m/s (right column); results for simulations run at 0.1 and 0.5 m/s given in the supplementary material. Results visualized as two-dimensional plots of flow-velocity magnitude with flow vectors (colored arrows; length of arrows scaled to 8× and 1.5× the flow-velocity magnitude for 0.05 and 0.2 m/s, respectively), in plan (upper panels) and lateral (lower panels) views. The ambient flow is from left to right.

Current Velocity

For all the simulations with a depth-averaged velocity of 0.05 m/s, flow moved in a streamlined fashion with little recirculation within the wake (Figs. 3, 4). For simulations with faster velocities (≥0.1 m/s), flow was recirculated in the wake immediately downstream of the triradial arms, developing a countercurrent that directed fluid toward the apex. For all the simulated current velocities, including 0.05 m/s, some degree of redirection was observed in the movement of flow above the pit that was located farthest upstream. The development of a small vortex above this

https://doi.org/10.1017/pab.2024.24 Published online by Cambridge University Press

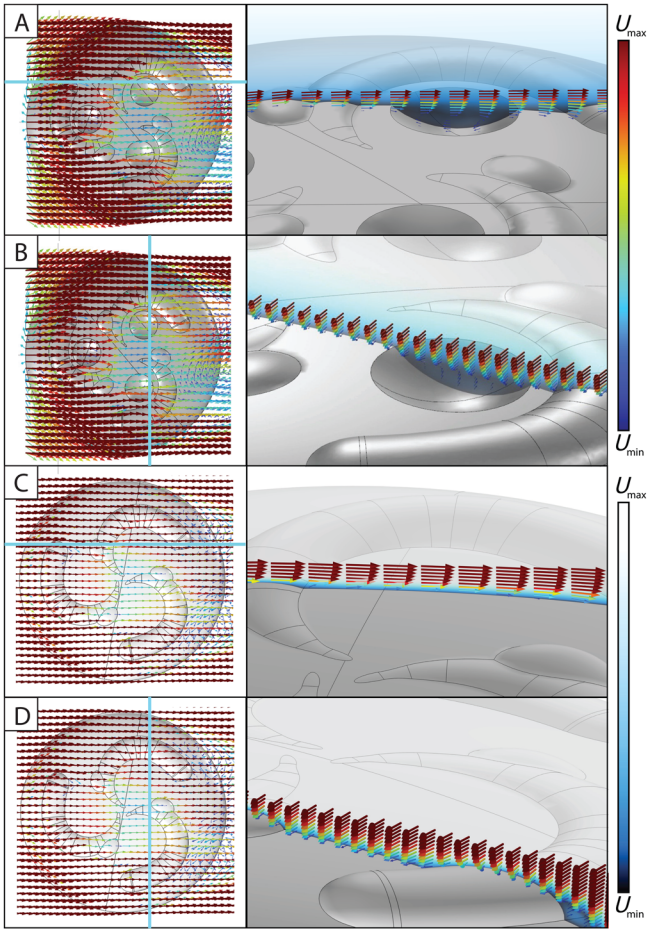

Figure 5. Close-up of flow patterns around the apex of *Tribrachidium* in oblique view, in models possessing bullae, with **(A, B)** and without **(C, D)** apical pits. Blue lines in left-hand panels illustrate the orientation of cut planes. Note in particular the movement of arrows in the opposite direction of ambient flow is more prevalent in the model including pits.

pit was most prominent for 0.1 and 0.2 m/s simulations, with 0.05 m/s simulations showing less deviation from the predominant direction of ambient flow and 0.5 m/s simulations developing a layer of fast-moving flow immediately above this region of recirculation.

Orientation

Changing the orientation of models with arms had some noticeable effects on the flow patterns. For example, the model rotated 40° relative to the default orientation slowed and recirculated fluid to some extent over all pits when inlet velocities were greater than 0.1 m/s, but did not redirect fluid from the wake to any of the apical pits. With the model rotated 80° relative to the default orientation, there was some redirection of flow from the wake toward the apex of the organism, but this pattern was weaker than in the simulations with models in the 0° orientation. Additionally, reduction in flow velocity and recirculation was evident for all three apical pits in this orientation. As noted earlier, at inlet velocities of ≤0.1 m/s, the flow was streamlined, with minor recirculation occurring over a small region behind the downstream arm, whereas at inlet velocities of ≥0.2 m/s, recirculation was stronger, albeit less so than what was observed for 0° orientation.

Group-Level Simulations

Flow features present in the complete model were also generated in the two group-level simulations (Fig. 6). Velocity slowed as flow approached the upstream model, with higher velocities restricted to fast-moving jets of fluid between the downstream models. Patterns of recirculation were broadly similar to those described for the individual *Tribrachidium* models. Recirculation within wakes was most noticeable at inlet velocities of 0.5 m/s in both the clumped and spaced arrangements. Coefficients of drag were calculated for all the models within both group arrangements, which showed similar values for both upstream and downstream models.

CFD-DEM Simulations

The trajectories of suspended particles were impacted substantially by the morphology of the *Tribrachidium* models and associated flow structures. Only particles with radii of ~100 µm and larger were deposited in our simulations, and only at flow velocities of $U = 0.02$ and 0.05 m/s. The size threshold of settling particles broadly reflects the Archimedes number:

$$Ar = \frac{[gr^3(\rho_p - \rho_f)]}{(\rho_f \upsilon^2)} \quad (1)$$

where g is the magnitude of gravitational acceleration; ρ_p and ρ_f are the particle and fluid densities, respectively; and υ is the kinematic viscosity of fluid), which is the ratio of resultant vertical force (gravity minus buoyancy) to viscous force. When $r > 109.3$ and $Ar > 1$, particles will be brought down to the substrate/organism under the influence of gravity. This means that only relatively large particles will be deposited in low-speed flows, consistent with the central tenets of sedimentology (Cao et al. 2005). Lower flow speeds will also intuitively lead to increased settling of particles; a phenomenon that can be quantified by the Froude number ($Fr = \frac{U}{\sqrt{2gr}}$), which describes the relative magnitude of inertia versus gravity.

We found that the number of particles settling in each apical pit, and the pathways to settling, differed substantially between the three apical pits in our models. Moreover, we found that these aspects changed with increasing simulated flow velocity. When $Fr \ll 1$, the deposition of particles with a radius of 100 µm was generally homogeneous along the path of fluid flow (reflecting the fact that gravity is strong relative to inertia), and flow paths to deposition within the pits were approximately straight (Fig. 7). However, due to the blocking effect of the left and upper arms, the fluid velocity in the right pit (as well as the furrow leading to the right pit) is lower, creating a relatively stagnant region for particles to settle. As a result, more particles settled in the right pit than in either of the two upstream pits, as shown in Figure 8A.

By contrast, when $Fr \approx 1$, the settling of particles was more heavily influenced by the morphology of *Tribrachidium*, and pathways to settling in the three pits were more curved. In the rightmost pit, fluid flow deviated at the end of the right furrow and formed a slowly recirculating vortex above the pit the velocity vector field and the z component of the vorticity field [$\omega = \nabla \times U$, where $\mathbf{U}$ is the fluid velocity vector field]. In this structure, the vorticity is relatively low compared with the left and upper pits, leading to a favorable environment for settling

https://doi.org/10.1017/pab.2024.24 Published online by Cambridge University Press

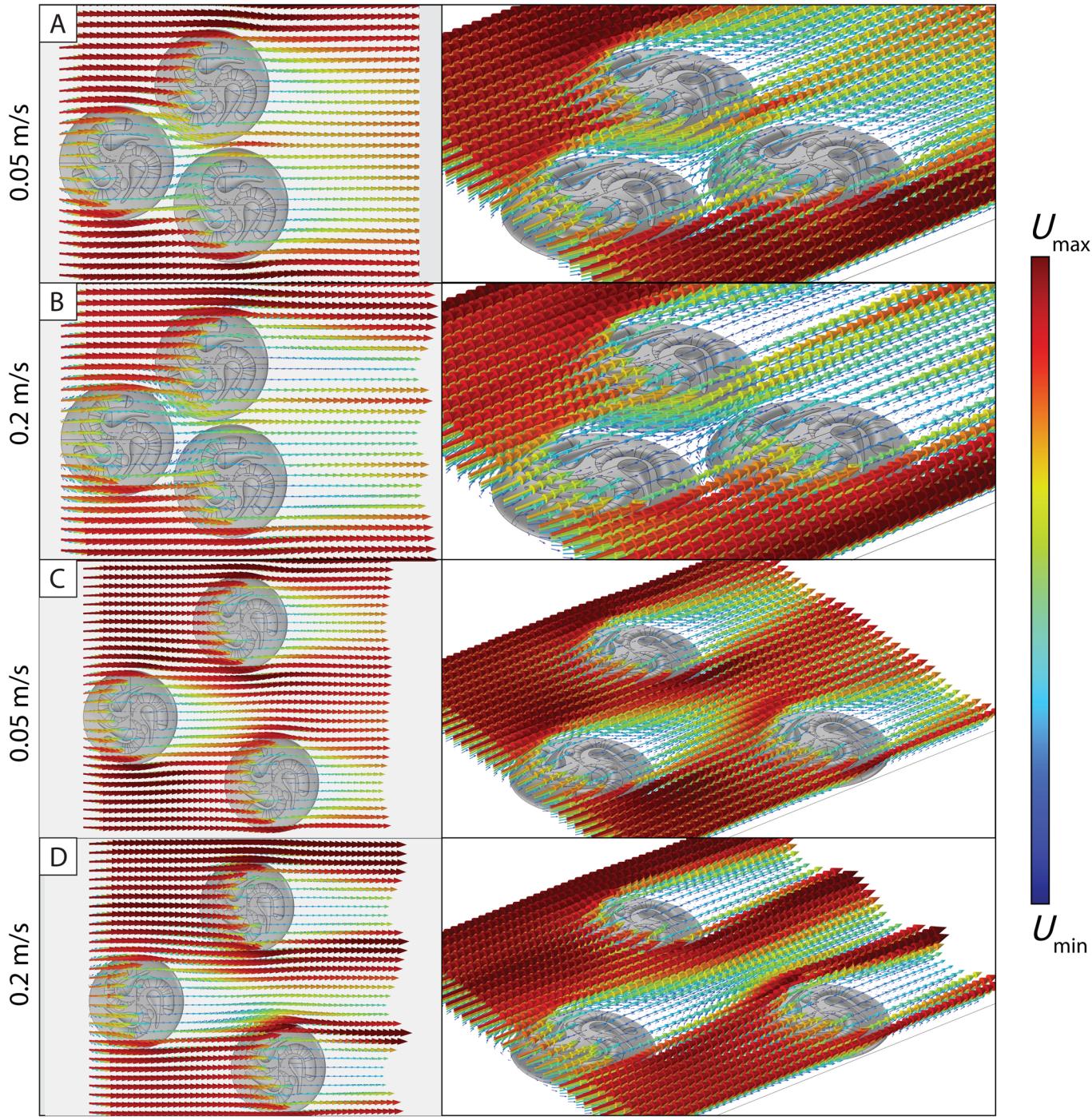

Figure 6. Results of group-level computational fluid dynamics (CFD) simulations, showing tightly spaced **(A, B)** and loosely spaced (**C, D)** aggregations of *Tribrachidium*, shown in plan (left panels) and oblique (right panels) views. Flow vectors given by the directions of arrows, and velocity magnitude given by both arrow size and color. The ambient flow is from left to right.

of particles. Nevertheless, virtually no particles settled in the left and right pits—the faster flow (and faster-rotating vortices) over the pits created a low-pressure zone and transported particles away downstream due to what are referred to as Saffman forces (Zhou et al. 2007). Some of the particles from the left pit eventually settled downstream in the right pits (orange lines in Fig. 7B) due to drag force deficiency in the decelerated flow regime and the downward deviated flow over the no-slip organismal surface. Some of the particles from the upper pit were carried away by the accelerated flow due to the narrower furrow. Therefore, the total number of trapped particles is determined by the particles caught by the right pit, as shown in Figure 8B. In conjunction with the strong recirculation seen in the wakes, numerous particles also accumulated immediately behind the models (Fig. 7B). Finally, when $Fr \gg 1$ (flow velocity 0.2 m/s) particles were entirely carried away by fluids and became suspended (Fig. 7C).

https://doi.org/10.1017/pab.2024.24 Published online by Cambridge University Press

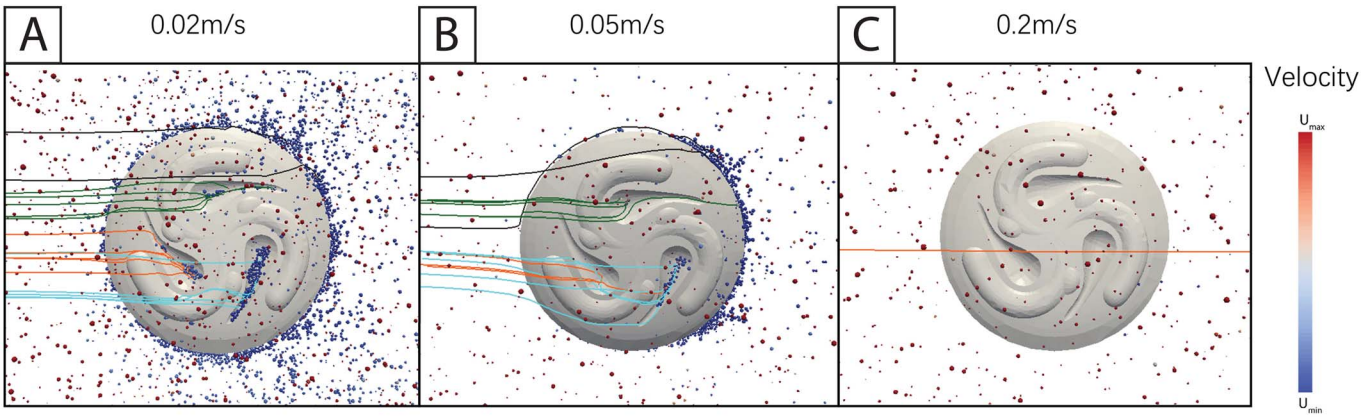

Figure 7. Typical trajectories of particles under three inflows: **(A)** 0.02 m/s, **(B)** 0.05 m/s, and **(C)** 0.20 m/s, modeled using computational fluid dynamics–discrete element method (CFD-DEM).

Contrasting Our Two "Complete" Models

Patterns differ slightly between our two "complete" models; however, the central hydrodynamic features remain consistent. Specifically, flow is slowed within the pits, and a slow-moving countercurrent is generated within them that flows in the opposite direction to that in the far field (Fig. 9). In terms of differences, the length of this region of recirculation was greater in our model possessing more elongate pits, and flow was more noticeably redirected. However, in more margin-ward areas where pits were less sheltered by the triradial arms, this recirculation was weaker. More differences emerge when we subject these models to analyses using particle tracing—in models possessing elongate pits, some particles falling into the upstream pit would become resuspended, and then be recaptured by the adjacent downstream pit (although this effect was only seen at our fastest current velocity—0.5 m/s).

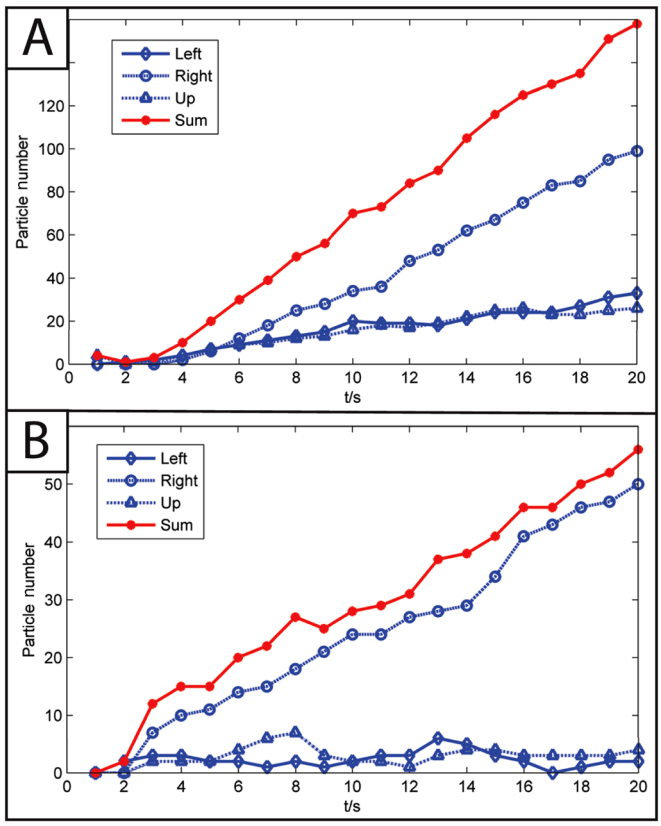

Figure 8. The particle-collection rate of different pits under $U = 0.02$ m/s **(A)** and $U = 0.05$ m/s **(B)**.

Discussion

The results obtained for our stepped series of hypothetical models reveal the potential roles played by specific anatomical features in producing flow patterns that may have helped *Tribrachidium* live in benthic communities. Broadly, our results support the inferences originally made by Rahman et al. (2015); fluid flow rapidly decreased in velocity where it first encountered our complete model, forming a low-velocity wake in the downstream area. In two of the three simulated model orientations, flow was redirected to the apex of the organism and entrained within small-scale vortices formed in the partially blocked apical pit; some degree of vortex generation was also observed over at least one other pit, depending on model orientation. This is consistent with a passive suspension-feeding lifestyle, in which flow would be expected to be redirected toward specific anatomical features (presumably those housing feeding structures; see Gibson et al. 2021a). Similar flow patterns are observed in extant sea anemones (Koehl 1977) and in association with the brachiopod lophophore (Vogel 1994). Our simulations also demonstrate that the triradial arms of *Tribrachidium* played a crucial role in slowing fluid flow and directing it up toward the apical pits, where low-velocity recirculation would have caused particles to fall out of suspension. This supports the inference that the apical pits originally housed feeding structures, although the precise mechanisms by which food particles would have been sorted, ingested, and digested remain speculative. Importantly, these patterns are consistent between both our individual- and group-level simulations, indicating that gregarious living would not have impeded feeding efficiency (although it equally would not have "enhanced" feeding, as has been demonstrated for the erniettomorph taxa *Ernietta* and *Pteridinium*; see Gibson et al. 2019, 2021a; Darroch et al. 2022).

Our CFD-DEM simulations add nuance to this picture, illustrating that the passive settling of particles in apical pits would have been maximized under conditions of relatively low *Fr* and high *Ar* numbers—that is, lower inertia and higher gravitational

https://doi.org/10.1017/pab.2024.24 Published online by Cambridge University Press

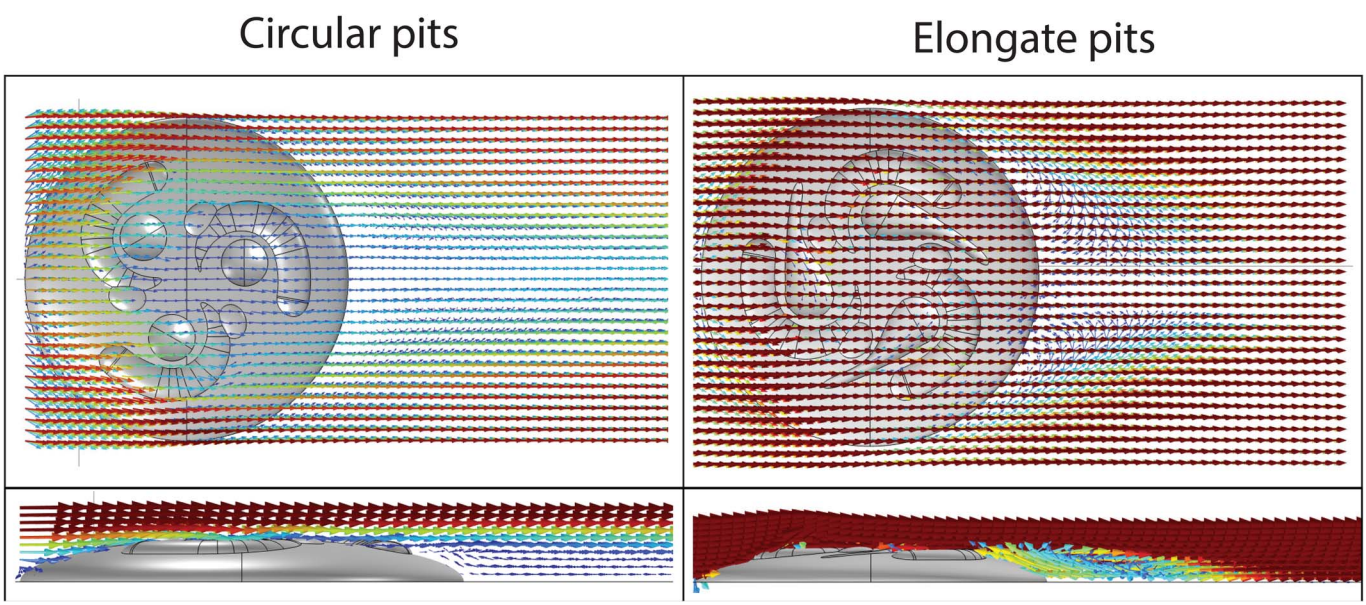

Figure 9. Illustrating flow patterns in our two different "complete" models, with circular pits (left panel) and elongate pits (right panel) under $U = 0.2$ m/s.

forces (heavier or larger particles)—and in specific orientations to flow. If $Fr \ll 1$, then particle deposition would have been relatively homogeneous along the direction of flow, and the number of particles "caught" would depend on the total size of the pits. If, however, $Fr \approx 1$, then particle motion would be more impacted by flow structures around individuals of *Tribrachidium*, leading to the settling of particles entrained in vortices downstream of the arms. The orientation of the organism is also key, as in orientations where the arms do not provide some shelter to the pit, no recirculation or particle deposition is possible. Consequently, particle-collection methods differed between the three apical pits, and moreover would have been different under varying flow regimes. Finally, when $Fr > 1$, particles would become suspended and not be deposited in pits. However, we also note that if *Fr* and Reynolds numbers (*Re*) were extremely high, then wall turbulence would be generated, along with cascading vortices of different scales. Under these circumstances, the behavior of particles would be dominated by inertia, meaning they would collide with the substrate and organism randomly—potentially increasing the particle capturing rate (assuming the existence of cilia, mucus membranes, or some other means of adhesion). These mechanisms of particle capture are different from those originally hypothesized by Rahman et al. (2015), who suggested that recirculated flow in the wake of organisms would have been the most important means by which particles were transported to pits.

We note that there are several methodological differences between our CFD study and that performed by Rahman et al. (2015). For example, those authors used a normal inflow velocity inlet that lacked a fully developed boundary layer, whereas our study used a fully developed flow inlet that a priori prescribes a law of the wall profile (see discussion in Gibson et al. 2021b). Furthermore, the digital model used by Rahman et al. (2015) was derived from a fossil specimen with morphological features deformed by taphonomic processes—for example, one of the triradial arms was longer than the other two—whereas our CAD model was geometrically regular. Finally, the model used by Rahman et al. (2015) inherently had surface texture that was absent from our purposefully idealized, smooth model surfaces. Despite these methodological differences, however, the flow patterns recovered by both studies are broadly consistent, and thus we are confident that macro- and mesoscale flow features seen in these simulations are an accurate depiction of what the organism would have experienced in life. In addition, the surface roughness from the Rahman et al. (2015) model indirectly provides insight into how *Tribrachidium* may have been affected by the textured organic surfaces that are often found associated with *Tribrachidium* fossils (Droser et al. 2019). Given the agreement in results between their textured surfaces and our infinitesimally smooth surfaces, such microbially textured surfaces would likely have only modified the relative position of the apical pits within the boundary layer—necessitating slower ambient velocities to guarantee particle deposition. While this prediction is consistent with the results presented here, a focused study assessing the influence of microbial mats and additional seafloor roughness on benthic flow fields is a crucial direction for future work.

Are Flow Patterns Dependent on Specific Anatomical Features?

The results of our analyses using a stepped series of hypothetical models demonstrate that certain anatomical features were essential to the formation of slow-moving, recirculated flow, which would have been conducive to suspension feeding via gravitational settling of particles. For example, the presence of the arms was key for the formation of a large wake (Figs. 3, 4), which redirected flow and particles over the model (depending on model orientation and current velocity). The inclusion of the apical pits was crucial for inducing a slow countercurrent of fluid that facilitated particle deposition. However, the precise shape of the reconstructed apical pits (i.e., hemispherical vs. elongate) did not appear to have a substantive impact on these flow patterns.

In contrast, our simulations show that the presence of bullae did not alter flow patterns in a way that would have influenced feeding; the only difference between simulation results for models with and without bullae was a localized shift in the direction of flow, which is unlikely to have greatly affected the number of

https://doi.org/10.1017/pab.2024.24 Published online by Cambridge University Press

food particles falling out of suspension at the hypothesized sites of particle capture. Previous authors have speculated that the bullae could have played a role in reproduction (Jenkins 1992), but our simulations do not support this interpretation. If the bullae were involved in releasing gametes, we would expect their shape to induce vertical flow such that gametes could more easily enter the water column to be distributed in the area surrounding the site of their release. However, by comparing the vertical component of velocity for models with and without bullae, we were able to determine that their presence did not noticeably affect vertical velocity.

CFD analysis of our stepped series of hypothetical models also allows us to address a crucial point surrounding the reconstructed morphology of *Tribrachidium* not addressed thus far—specifically, disagreements surrounding which of the prominent features studied here represent internal, rather than external anatomy. Ivantsov and Zakrevskaya (2021) have argued that the primary triradial arms and bullae of *Tribrachidium* represent entirely internal features, taking as evidence differences in the preserved heights and relative positions of these features in large versus small individuals. In this reconstruction, only the tentacular fringe would remain as a true external feature of the living organism (Ivantsov and Zakrevskaya [2021] also interpret the apical pits as internal, but acknowledge that they would have been linked to "oral openings," which presumably would also represent negative features). While physical evidence for this reconstruction is limited—the observations are apparently based on only two specimens, and the consistency with which these features are preserved (in particular among different facies and sediment types in South Australia and Russia) indicates that differential taphonomic compaction is a far more likely explanation—our study nonetheless allows us to evaluate to what extent this reconstruction affects our interpretations. Crucially, our results illustrate that in the absence of triradial arms, there would have been little wake formation, recirculation, or other flow features that would have led to the settling of particles on or around the model. Likewise, in the absence of apical pits, there would have been no generation of the slow countercurrents that led to the deposition of particles at the top of the organism. The presence of a tentacular fringe most likely had a negligible impact on broadscale flow patterns around the organism; however, if the grooves of this fringe were ciliated and capable of moving food toward the oral openings (see Ivantsov and Zakrevskaya [2021] and "Functional Morphology of *Tribrachidium* and the Broader Triradialomorpha" section), then particles deposited in the lee of the organism could still have been an important food source.

Tribrachidium *Group CFD*

A recent statistical analysis of in situ fossil assemblages in the Nilpena Ediacara National Park fossil site demonstrated that *Tribrachidium* lived both as isolated individuals and as aggregated Thomas clusters (Boan et al. 2023). The authors concluded that the spatial arrangement and aggregation of *Tribrachidium* were likely a consequence of favorable recruitment conditions with little postsettlement filtering. Rahman et al. (2015) hypothesized that denser populations of *Tribrachidium* may have created conditions favorable for consistent resuspension of nutrient particles—similar to what has been described for *Ernietta* (Gibson et al. 2019)—but they were constrained by computational resources and thus unable to directly test this hypothesis. We address this knowledge gap here.

Our group-level simulations demonstrate that the flow patterns associated with an individual model persisted when multiple models were included (approximating aggregation of individuals). Unlike erniettomorph taxa, for which group-level CFD results have shown that downstream individuals often experienced increased levels of turbulent mixing (Gibson et al. 2019, 2021a,b; Darroch et al. 2022), downstream *Tribrachidium* do not appear to have been exposed to much greater levels of mixing. Instead, turbulent kinetic energy (k) values are larger downstream from the aggregate, and the drag coefficients were fairly consistent between upstream and downstream models, with disparities present only at the fastest (0.5 m/s) inlet velocity. By way of contrast, *Ernietta* drag coefficients varied by orders of magnitude between upstream and downstream individuals (Gibson et al. 2019). These differences in mixing and drag values are most likely due to morphological variability between the "cavity"-type body plans of erniettomorphs and the hemispherical body plan of *Tribrachidium*. This illustrates that a hemispherical body shape streamlines flow and reduces drag, supporting the inference that *Tribrachidium* was capable of functioning in a variety of flow environments (Boan et al. 2023). This latter point is crucial, as *Tribrachidium* has been found to have functioned in communities that include taxa with greater relief above the seafloor (Hall et al. 2015) and that would therefore be expected to disrupt boundary layer flow.

Functional Morphology of Tribrachidium *and the Broader Triradialomorpha*

Our proposed feeding model for *Tribrachidium* allows us to speculate on feeding modes of other radial and triradial Ediacaran taxa, which are characterized by morphological variations on a common body plan. The Triradialomorpha comprise the (mostly) monospecific genera *Anfesta*, *Albumares*, *Rugoconites*, *Hallidaya*, *Skinnera*, and *Tribrachidium* (Hall et al. 2020); among these other taxa there are counterparts of the specific morphological features identified in this study as being potentially crucial to suspension feeding in *Tribrachidium*. However, there are obvious distinctions between these analogous features that may hint at different functions and ecological niches within White Sea-aged ecosystems.

Our analyses identify the triradial arms as being the single most important feature that leads to particle settlement in *Tribrachidium*. In addition, we identify the apical pits as likely sites of nutrient collection—both our and Rahman et al.'s (2015) CFD simulations and our CFD-DEM results demonstrate that the shape and orientation of the arms would have led to the settling of food particles in the three hemispherical depressions located toward the apex of the organism (but see the caveats surrounding internal vs. external morphology discussed earlier). Among the triradialomorphs, there is significant variation in these two facets of morphology that would have impacts on flow patterns and thus, presumably, the rates and styles of particle capture in different flow regimes. *Rugoconites*, *Anfesta*, and *Albumares* are similar-sized taxa all possessing straight, rather than curved, ridges that radiate from the center of the organism, terminating either at or shortly before the margin (Hall et al. 2020). The lack of torsional symmetry these taxa (excluding *Tribrachidium*) exhibit would thus seem to be at least as efficient at creating flow patterns that lead to particle settlement, although the degree to which this might be dependent on different ambient flow regimes (different velocities, mono-directional vs. oscillating

https://doi.org/10.1017/pab.2024.24 Published online by Cambridge University Press

flow, etc.) requires further testing. Moreover, *Rugoconites* seems to have differentiated primary arms through ontogeny in sets of 3, such that the smallest individuals have 3 primary arms, whereas larger individuals can possess 6, 9, or even 12 (although in 1 species, *Rugoconites tenuirugosus*, these arms tend to have minimal relief; see Hall et al. 2018, 2020). If the primary hydrodynamic function of the radial arms was to create areas of low-velocity recirculation above the apex of the organism (as suggested by our simulations), then we hypothesize that a higher number of arms would create slower and more complex flow patterns, ultimately leading to the settlement of more particles and thus supporting the growth of larger individuals. Interestingly, the taxa *Hallidaya* and *Skinnera* do not possess any arm-analogue structures (although they do possess apical pits), and so it is unclear to what extent the particle capture mechanism we outlined for *Tribrachidium* would have worked for these genera. It is conceivable that small-scale recirculation may have been generated in the pits under very low ambient flow velocities (see earlier discussion surrounding the behavior of particles under varying Froude numbers), although this remains to be tested. *Tribrachidium* is potentially an example of an ecological generalist—found in a wide variety of shallow-marine environments and possessing a morphology that apparently allowed it to feed irrespective of orientation to current (Rahman et al. 2015)—whereas related taxa (in particular *Skinnera* and *Hallidaya*) apparently have a much more limited geographic and paleoenvironmental distributions (Hall et al. 2020). It may be that these other, non-torsional triradial morphologies allow for suspension feeding under a much narrower set of conditions, thus making them comparatively more specialized. A related question surrounds the feeding mode of juvenile *Tribrachidium*, which were smaller, lived lower down within the turbulent boundary layer (potentially buffer or transition layer), and apparently lacked triradial arms and bullae (although they likewise possess apical pits; see Ivantsov and Zakrevskaya 2021); all of which would have meant a significantly different feeding style during later ontogeny. The emergence of suspension feeding among triradialomorphs is therefore potentially interesting from an evolutionary (as well as ecological) perspective, although there is as yet no published phylogeny for this group.

The number and arrangement of the apical pits is another character that varies among triradialomorph taxa. *Albumares*, *Anfesta*, and *Skinnera* all possess depressions toward their apices that represent structures potentially homologous to those seen in *Tribrachidium*. *Albumares*, *Anfesta*, and *Skinnera* all resemble *Tribrachidium* in that the pits are equidistant (i.e., reflect the symmetry state of the organism). The presence or absence of primary arms (which created flow patterns conducive to particle settling) notwithstanding, we hypothesize that the anatomical scheme observed in these taxa is compatible with similar feeding mechanisms to that proposed for *Tribrachidium*. *Hallidaya* is exceptional in that the number of pits (termed "nuclei" by Wade [1969]) is apparently plastic, with up to seven pits placed irregularly near the apex; however, this does not necessarily preclude a feeding mode similar to those of other triradialomorphs. *Rugoconites* lacks pits entirely, and thus—if pits represent sites of particle capture (potentially even oral openings)—we might envisage some other method of capture/ingestion.

Finally, all triradialomorphs possess radiating linear indentations ("grooves") in their upper surface, a feature frequently referred to as the "tentacular fringe" in *Tribrachidium* (e.g., Rahman et al. 2015). These grooves typically originate at the pits, and branch (sometimes multiple times) as they extend out toward the perimeter of the organism. In *Rugoconites* and *Anfesta*, these grooves follow straight paths and terminate at the body perimeter, whereas in *Hallidaya*, the grooves terminate at an inner raised "rim" close to the body margin. In *Skinnera*, the grooves are shorter and apparently connect with a secondary ring of 15 smaller pits that surround a central grouping of three primary apical pits. It was not computationally feasible to incorporate grooves into our *Tribrachidium* models used in CFD analyses, and so we are unable to comment on their impact on flow patterns. We can, however, speculate as to the role they may have played in feeding. Previous authors have speculated that the outer surface of *Tribrachidium* could have been covered in cilia for the purpose of capturing suspended particles and transporting them to feeding sites (Ivantsov and Zakrevskaya 2021). Given that grooves appear to terminate at the apical pits in many studied triradialomorph taxa (Hall et al. 2020), if these grooves were ciliated, then it is conceivable they may have been used to transport food particles deposited in the immediate wake of the organism—something suggested by our particle-tracing results—toward the feeding apparatus at the apex.

In summary, our study allows us to reconstruct a plausible feeding mode for *Tribrachidium* that may also be applicable to a broader grouping of triradialomorph taxa that flourished in shallow-marine environments during the late Ediacaran White Sea interval. Our results provide support for a model wherein apical pits represented loci of particle collection (and possibly ingestion), the primary triradial arms interrupted ambient flow and helped create the hydrodynamic conditions required for particle settling (and thus adaptations to higher-energy flow regimes), and—more speculatively—radial grooves represented ciliated conduits that may have transported food particles accumulating in the wake of the organism toward apical pits. In this scenario, morphological variation among different members of the Triradialomorpha might represent variations on this theme. For example, taxa with more prominent arms may have been better adapted to higher-energy environments, while those with no arms (but with more pits and a more elaborate arrangement of pits) may have been better adapted to lower-energy environments. Conversely, one could imagine that variations in triradial anatomy may have prevented these other body plans from capturing particles effectively at all. Further investigation is needed to determine whether a suspension-feeding interpretation can be applied to triradialomorphs more broadly. This is testable with: (1) CFD analysis of more triradial taxa; (2) detailed facies analysis of sediments hosting different genera; and (3) reexamination of well-preserved specimens. If correct, such a model would also suggest that the White Sea interval was characterized by a major evolutionary radiation of low-tier benthic suspension feeders, indicating a diversity of ecological niches that apparently decreased in the subsequent Nama interval ~548–538 Ma (see, e.g., Darroch et al. 2022).

Conclusions

Our CFD and CFD-DEM simulations allow us to probe the functional morphology of *Tribrachidium*, informing on the role played by specific anatomical features in supporting a suspension-feeding lifestyle. Specifically, our results provide strong support for interpreting *Tribrachidium* as an Ediacaran macroscopic suspension feeder, with apical pits representing the loci of particle collection (and possibly ingestion), and triradial arms representing morphological adaptations for interrupting flow and inducing settling of

https://doi.org/10.1017/pab.2024.24 Published online by Cambridge University Press

particles. Our population simulations show that denser populations were unlikely to enhance the feeding efficiency of *Tribrachidium* individuals through resuspension of nutrient particles without the adoption of an active feeding style, as speculated by Ivantsov and Zakrevskaya (2021). *Tribrachidium*'s body shape was adapted to surviving in variable-flow conditions, permitting it to live as either an isolated individual or as a member of a larger population. Unlike erniettomorphs that experienced varying degrees of turbulent mixing depending on their location within an aggregate, *Tribrachidium* individuals experienced similar flow conditions regardless of their position.

Our experiments using particle tracing via CFD-DEM add considerable nuance to the scenario originally hypothesized by Rahman et al. (2015); whereas this previous study suggested that the primary method of particle settling would have been by recirculation of flow in the wake of the organism, our experiments show that passive settling of particles in apical pits would have primarily been in the lee of the arms and was maximized under conditions of relatively low *Fr* and high *Ar* numbers. Consequently, the methods and efficiency of particle-collection methods would have varied among the three apical pits and, moreover, would have been sensitive to changing flow regimes. Finally, particle-tracing experiments show that a large number of particles would have accumulated in the wake of the organism, adjacent to the margin. We speculate that the radial grooves (or tentacular fringe) of *Tribrachidium* may represent ciliated pathways through which these food particles could be transported toward apical pits.

Our results allow us to generate new hypotheses surrounding homologous structures shared with other Ediacaran triradial taxa, which may also have played a role in feeding. This work refines our understanding of the appearance of suspension feeding in shallow-water paleoenvironments, with implications for the radiation of Metazoa over the Ediacaran/Cambrian boundary.

Acknowledgments. This research was supported by joint funding from the U.S. National Science Foundation (NSF-NERC EAR-2007928) and the UK Natural Environment Research Council (NE/V010859/2). S.A.F.D. and R.A.R. acknowledge generous support from the Alexander von Humboldt Foundation, which is sponsored by the Federal Ministry for Education and Research (Germany). A.O. was funded by the Searle Undergraduate Research Program ("SYBBURE"), and this research was performed in partial fulfillment of a senior thesis at Vanderbilt University. B.M.G. acknowledges computational support from two Vanderbilt University Alberstadt, Reeseman, and Sterns grants, and a University of Toronto Mississauga postdoctoral fellowship. F.S.D. acknowledges additional support from the Royal Commission for the Exhibition of 1851, Merton College, Oxford, and an independent research fellowship from the Natural Environment Research Council (NE/W00786X/1). Z.W. acknowledges funding from the Royal Society and the K.C. Wong Education Foundation. S.A.F.D. and R.A.R. thank Mary-Ann Binnie for allowing access to fossil specimens housed at the South Australia Museum. This article was significantly improved after constructive comments from two anonymous reviewers.

Competing Interest. The authors declare no competing interests.

Data Availability Statement. The 3D models, CFD simulation setups, and all supplementary materials are available from Dryad https://doi.org/10.5061/dryad.dr7sqvb65.

Literature Cited

Boag, T. H., S. A. F. Darroch, and M. Laflamme. 2016. Ediacaran distributions in space and time: testing assemblage concepts of earliest macroscopic body fossils. *Paleobiology* **42**:574–594.

Boan, P., S. Evans, C. Hall, and M. Droser. 2023. Spatial distributions of *Tribrachidium*, *Rugoconites*, and *Obamus* from the Ediacara Member (Rawnsley Quartzite), South Australia. *Paleobiology* **49**:601–620.

Brocks, J. J., A. J. M. Jarrett, E. Sirantoine, C. Hallmann, Y. Hoshino, and T. Liyanage. 2017. The rise of algae in Cryogenian oceans and the emergence of animals. *Nature* **548**:578–581.

Butterfield, N. J. 2022. Constructional and functional anatomy of Ediacaran rangeomorphs. *Geological Magazine* **1597**:1148–1159.

Cao, Z. X., G. Pender, and J. Meng. 2005. Explicit formulation of the Shields diagram for incipient motion of sediment. *Journal of Hydraulic Engineering* **132**:1097–99.

Cracknell, K., D. C. García-Bellido, J. G. Gehling, M. J. Ankor, S. A. F. Darroch, and I. A. Rahman. 2021. Pentaradial eukaryote suggests expansion of suspension feeding in White Sea-aged Ediacaran communities. *Scientific Reports* **11**:4121.

Darroch, S. A. F., E. F. Smith, M. Laflamme, and D. H. Erwin. 2018. Ediacaran extinction and Cambrian explosion. *Trends in Ecology and Evolution* **33**:653–663.

Darroch, S., B. Gibson, M. Syversen, I. Rahman, R. Racicot, F. Dunn, S. Gutarra, E. Schindler, A. Wehrmann, and M. Laflamme. 2022. The life and times of *Pteridinium simplex*. *Paleobiology* **48**:527–556.

Droser, M. L., and J. G. Gehling, J. G. 2015. The advent of animals: the view from the Ediacaran. *Proceedings of the National Academy of Sciences USA* **112**:4865–4870.

Droser, M. L., J. G. Gehling, L. G. Tarhan, S. D. Evans, C. M. S. Hall, I. V. Hughes, E. B. Hughes, *et al.* 2019. Piecing together the puzzle of the Ediacara Biota: excavation and reconstruction at the Ediacara National Heritage site Nilpena (South Australia). *Palaeogeography, Palaeoclimatology, Palaeoecology* **513**:132–145.

Dynowski, J. F., J.H. Nebelsick, A. Klein, and A. Roth-Nebelsick. 2016. Computational fluid dynamics analysis of the fossil crinoid *Encrinus liliiformis* (Echinodermata: Crinoidea). *PLoS ONE* **11**:e0156408.

Fedonkin, M. A. 1985. Precambrian metazoans: the problems of preservation, systematics and evolution. *Philosophical Transactions of the Royal Society B* **311**:27–45.

Gehling, J. G., and M. L. Droser. 2013. How well do fossil assemblages of the Ediacara Biota tell time? *Geology* **41**:447–450.

Gibson, B. M., I. A. Rahman, K. M. Maloney, R. A. Racicot, H. Mocke, M. Laflamme, and S. A. F. Darroch. 2019. Gregarious suspension feeding in a modular Ediacaran organism. *Science Advances* **5**:eaaw0260.

Gibson, B. M., S. A. F. Darroch, K. M. Maloney, and M. Laflamme. 2021a. The importance of size and location within gregarious populations of *Ernietta plateauensis*. *Frontiers in Earth Science* **9**. https://doi.org/10.3389/feart.2021.749150.

Gibson, B. M., D. J. Furbish, I. A. Rahman, M. W. Schmeeckle, M. Laflamme, and S. A. F. Darroch. 2021b. Ancient life and moving fluids. *Biological Reviews* **96**:129–152.

Gili, J., and R. Coma. 1998. Benthic suspension feeders: their paramount role in littoral marine food webs. *Trends in Ecology and Evolution* **13**:316–321.

Grazhdankin, D. 2014. Patterns of evolution of the Ediacaran soft-bodied biota. *Journal of Paleontology* **88**:269–283.

Hall, C. M. S., M. L. Droser, J. G. Gehling, and M. E. Dzaugis. 2015. Paleoecology of the enigmatic *Tribrachidium*: new data from the Ediacaran of South Australia. *Precambrian Research* **269**:183–194.

Hall, C. M., M. L. Droser, and J. G. Gehling 2018. Sizing up "Rugoconites": A study of the ontogeny and ecology of an enigmatic Ediacaran genus. *Australasian Palaeontological Memoirs* **51**, https://search.informit.org/doi/10.3316/informit.281736230240570

Hall, C. M. S., M. L. Droser, E. C. Clites, and J. G. Gehling. 2020. The short-lived but successful tri-radial body plan: a view from the Ediacaran of Australia. *Australian Journal of Earth Sciences* **67**:885–895.

Ivantsov, A. Y., and M. A. Zakrevskaya. 2021. Trilobozoa, Precambrian tri-radial organisms. *Paleontological Journal* **55**:727–741.

Jenkins, R. J. F. 1992. Functional and ecological aspects of Ediacaran assemblages. Pp. 131–176 *in* J. H. Lipps and P. W. Signor, eds. *Origin and early evolution of the Metazoa*. Topics in Geobiology 10. Springer, Boston.

Klein, H., and E. Mittelstaedt. 1991. Local currents at a shoreface-connected ridge in the German Bight. *Deutsche Hydrographische Zeitschrift* **44**:133–142.

https://doi.org/10.1017/pab.2024.24 Published online by Cambridge University Press

Klein, H., P. König, and A. Frohse. 1999. Currents and near-bottom suspended matter dynamics in the central north sea during stormy weather—results of the PIPE'98 field experiment. *Deutsche Hydrographische Zeitschrift* **51**:47–66.

Koehl, M. A. R. 1977. Effects of sea anemones on the flow forces they encounter. *Journal of Experimental Biology* **69**:87–105.

LaBarbera, M. 1984. Feeding currents and particle capture mechanisms in suspension feeding animals. *American Zoologist* **24**:71–84.

Lerosey-Aubril, R., and S. Pates. 2018. New suspension-feeding radiodont suggests evolution of microplanktivory in Cambrian macronekton. *Nature Communications* **9**:3774.

Loth, E., and A. J. Dorgan. 2009. An equation of motion for particles of finite Reynolds number and size. *Environmental Fluid Mechanics* **9**:187–206.

Mei, R. 1992. An approximate expression for shear lift force on a spherical particle at a finite Reynolds number. *International Journal of Multiphase Flow* **18**:145–147.

Rahman, I. A., S. A. F. Darroch, R. A. Racicot, and M. Laflamme. 2015. organismal biology: suspension feeding in the enigmatic Ediacaran organism *Tribrachidium* demonstrates complexity of Neoproterozoic ecosystems. *Science Advances* **1**:e1500800.

Schlichting, H., and K. Gersten. 2000. *Boundary-layer theory*. Springer, Berlin.

Vogel, S. 1994. *Life in moving fluids: the physical biology of flow*. Princeton University Press, Princeton, N.J.

Wade, M. 1969. Medusae from uppermost Precambrian or Cambrian sandstones, central Australia. *Palaeontology* **12**:351–365.

Waggoner, B. 2003.The Ediacaran Biotas in space and time. *Integrative and Comparative Biology* **43**:104–113.

Wang, D., H. Ling, U. Struck, X. Zhu, M. Zhu, T. He, B. Yang, A. Gamper, and G. A. Shields. 2018. Coupling of ocean redox and animal evolution during the Ediacaran–Cambrian transition. *Nature Communications* **9**:2575.

Wang, Z. K., Y. J. Teng, and M. B. Liu. 2019. A semi-resolved CFD-DEM approach for particulate flows with kernel based approximation and Hilbert curve based searching strategy. *Journal of Computational Physics* **384**:151–169.

Wood, R., and A. Curtis. 2014. Extensive metazoan reefs from the Ediacaran Nama Group, Namibia: the rise of benthic suspension feeding. *Geobiology* **13**:112–122.

Zbib, H., M. Ebrahimi, F. Ein-Mozaffari, and A. Lohi. 2018. Comprehensive analysis of fluid-particle and particle-particle interactions in a liquid-solid fluidized bed via CFD-DEM coupling and tomography. *Powder Technology* **340**:116–130.

Zhou, X. Y., H. Cheng, C. L. Zhang, and Y. Z. Zhao. 2007. Effects of the Magnus and Saffman forces on the saltation trajectories of sand grain. *Geomorphology* **90**:11–22.

https://doi.org/10.1017/pab.2024.24 Published online by Cambridge University Press